Biochimica et Biophysica Acta 1808 (2011) 271–278

Contents lists available at ScienceDirect

Biochimica et Biophysica Acta

journal homepage: www.elsevier.com/locate/bbamem

α-Hemolysin pore formation into a supported phospholipid bilayer using cell-free expression

Jerome Chalmeau [a,b,c], Nadezda Monina [c], Jonghyeon Shin [c], Christophe Vieu [a,b], Vincent Noireaux [c,*]

[a] CNRS, LAAS, 7 avenue du Colonel Roche, F-31077 Toulouse, France
[b] Université de Toulouse ; UPS , INSA , INP, ISAE ; LAAS ; F-31077, Toulouse, France
[c] Physics Department, University of Minnesota, Minneapolis, MN, USA

ARTICLE INFO

Article history:
Received 2 June 2010
Received in revised form 19 July 2010
Accepted 26 July 2010
Available online 6 August 2010

Keywords:
Cell-free expression
α-hemolysin
Quartz crystal microbalance-dissipation
Fluorescence microscopy

ABSTRACT

Cell-free protein synthesis is becoming a serious alternative to cell-based protein expression. Cell-free systems can deliver large amounts of cytoplasmic recombinant proteins after a few hours of incubation. Recent studies have shown that membrane proteins can be also expressed in cell-free reactions and directly inserted into phospholipid membranes. In this work, we present a quantitative method to study in real time the concurrent cell-free expression and insertion of membrane proteins into phospholipid bilayers. The pore-forming protein α-hemolysin, fused to the reporter protein eGFP, was used as a model of membrane protein. Cell-free expression of the toxin in solution and inside large synthetic phospholipid vesicles was measured by fluorometry and fluorescence microscopy respectively. A quartz crystal microbalance with dissipation was used to characterize the interaction of the protein with a supported phospholipid bilayer. The cell-free reaction was directly incubated onto the bilayer inside the microbalance chamber while the frequency and the dissipation signals were monitored. The presence of pores in the phospholipid bilayer was confirmed by atomic force microscopy. A model is presented which describes the kinetics of adsorption of the expressed protein on the phospholipid bilayer. The combination of cell-free expression, fluorescence microscopy and quartz crystal microbalance-dissipation is a new quantitative approach to study the interaction of membrane proteins with phospholipid bilayers.

1. Introduction

Originally developed to study transcription and translation processes, cell-free systems are now used in many studies ranging from molecular level to large scale experiments [1]. Cell-free expression allows the production of a large quantity of proteins in a few hours. *In vitro* synthesis of proteins is faster and easier than cell-based recombinant protein preparation. Cell-free expression, which includes the transcription and the translation steps, only necessitates molecular cloning and eliminates protein purification procedures. Recently, different types of membrane proteins were successfully expressed in cell-free reactions. The pore-forming protein α-hemolysin was expressed inside large synthetic phospholipid vesicles to create a long-lived artificial cell system [2]. Cell-free expression of the toxin was also used to study the electrical properties of the pore [3]. The interaction of cell-free synthesized G-protein coupled receptors with a planar phospholipid bilayer was described qualitatively [4]. Integral membrane proteins were directly inserted into the lipidic bilayer of small unilamellar vesicles [5,6]. These works represent considerable technical advances for membrane protein studies as well as a promising alternative to cell-based membrane protein preparation. However, quantitative experimental approaches to characterize the concurrent expression and insertion of membrane proteins have not been proposed. The development of methods to study membrane protein expression using cell-free systems is highly desirable since interactions and self-assembly of proteins into phospholipid bilayers are essential biophysical processes in living cells. In this work a quantitative method is presented to study the interaction of the protein α-hemolysin from *Staphylococcus aureus*, synthesized in a cell-free extract, with a phospholipid membrane. The fusion protein αHL-eGFP was expressed through a transcriptional activation cascade inside large phospholipid vesicles and on an SPB. Expression kinetics, protein concentration and activity were measured by fluorometry and fluorescence microscopy. A QCM-D monitoring technique was used to characterize the adsorption of the pore-forming protein on an SPB.

α-hemolysin, a toxin secreted by *Staphylococcus aureus*, is a typical membrane pore-forming protein [7]. The toxin, produced as a water-soluble monomeric 293-residue protein, forms heptameric channels in

Abbreviations: QCM-D, quartz crystal microbalance-dissipation; SPB, supported phospholipid bilayer; AFM, atomic force microscopy; eGFP, enhanced Green Fluorescent Protein; αHL-eGFP, α-hemolysin-eGFP fusion protein; PBS, phosphate buffered saline; EggPC, L-α-lysophosphatidylcholine; POPC, 1-palmitoyl-2-oleoyl-*sn*-glycero-3-phosphatidylcholine; Δ*f*, frequency shift; Δ*D*, dissipation shift

* Corresponding author.
E-mail address: noireaux@umn.edu (V. Noireaux).

0005-2736/$ – see front matter © 2010 Elsevier B.V. All rights reserved.
doi:10.1016/j.bbamem.2010.07.027

phospholipid membranes without the assistance of any other molecules. Due to its pore of nanometer size and its hydrophilicity, α-hemolysin has been studied as a model of ionic channel and protein self-assembly in phospholipid bilayers.

The QCM-D technology is a sensitive technique to study molecular interactions on surfaces, SPB in particular. The working principle of the QCM-D technique is based on the piezoelectric properties of quartz. A quartz crystal sensor is actuated at high frequency and its mechanical oscillations are recorded. When the sensor mass changes, due to adsorption or desorption of molecules, a shift of the resonance frequency is observed which is proportional to the mass adsorbed on or desorbed from the sensor surface. The QCM-D technique allows real time quantitative measurements of mass changes on the sensor surface. In addition to frequency, the dissipation signal, which monitors the energy loss in the mechanical oscillations, provides information related to the viscoelastic properties of the adsorbed material. First developed for thin film deposition in vacuum, the QCM-D technique is now used routinely to monitor SPB formation [8], SPB interactions [9], protein-protein interactions [10], cell-surface interactions [11] and adsorption of proteins on SPB [12]. Recently, the QCM-D technique, combined with electrochemical impedance spectroscopy, was used to study the insertion of the pore-forming peptide gramicidin D [13]. In the present study, we show that cell-free expression of αHL-eGFP can be carried out directly on an SPB inside the QCM-D chamber. A Δf of more than 150 Hz was observed in the first 30 min of expression. A large ΔD was also observed, indicating a change in the viscoelastic properties of the bilayer. The presence of αHL-eGFP pores was confirmed by AFM in a liquid environment. A lower limit of the protein association constant on the SPB was found with an adsorption kinetics model. The experimental approach presented in this work could be extended to other membrane proteins that can be synthesized by cell-free extracts [6].

2. Materials and methods

2.1. Cell-free reaction

The crude extract was prepared with *Escherichia coli* BL21 Rosetta2 cells according to Shin and Noireaux [14]. Briefly, the S30 buffer A (5 mM Tris, 60 mM potassium glutamate and 14 mM magnesium glutamate, pH 7.7, 2 mM DTT) was used for washing and resuspension. Cells were broken with a bead beater (mini bead-beater-1, Biospecs Products Inc, Bartlesville, OK). The crude extract was dialyzed against the S30 buffer B (5 mM Tris, 60 mM potassium glutamate and 14 mM magnesium glutamate, pH 8.2, 1 mM DTT). The crude extract was stored at −80 °C after dialysis. The cell-free reaction was composed of 33% crude extract, the other 66% containing plasmids and the following components: 50 mM Hepes pH 7.6, 1.5 mM ATP and GTP each, 0.9 mM CTP and UTP each, 1 mM spermidine, 0.75 mM cAMP, 0.33 mM NAD, 0.26 mM coenzymeA, 30 mM 3-phosphoglyceric acid, 0.068 mM folinic acid, 0.2 mg/ml tRNA, 1 mM IPTG, 1 mM each amino acids, 2% PEG 8000, 2 mM magnesium glutamate, 60 mM potassium glutamate. The endogenous *E. coli* RNA polymerase was used for expression.

2.2. Plasmids

All the plasmids used in the study were constructed from the plasmid pBEST-Luc (Promega Corporation, Madison, WI). *E. coli* sigma factor 28 was cloned under a PtacI promoter (plasmid PtacI-sigma28, 0.5 nM final concentration). The reporter protein eGFP and the fusion protein αHL-eGFP (2) were cloned under a Ptar promoter specific to the *E. coli* sigma factor 28 [15]. The plasmids Ptar-eGFP and Ptar- αHL-eGFP were used at a final concentration of 5 nM.

2.3. Fluorescence measurements

A PerkinElmer Wallac Victor III plate reader was used to measure expression of eGFP and αHL-eGFP in solution. An Olympus IX71 inverted microscope equipped with a QImaging Retiga camera was used to measure αHL-eGFP fluorescence inside large vesicles. Pure recombinant eGFP (Clontech, Mountain View, CA) was used to calibrate and quantify fluorescence. Cell-free expression inside large phospholipid vesicles (EggPC, Avanti Polar Lipids, Alabaster, AL) was performed as described previously [2]. After formation, the large vesicles were placed between two microscope cover glasses with a spacer of 250 μm. The vesicles fall by sedimentation on the bottom cover glass where they stay stationary.

2.4. Supported phospholipid bilayer

POPC phospholipids (Avanti Polar lipids, Alabaster, AL) were stored at −20 °C before dilution in pure chloroform at a concentration of 1 mg/ml. Chloroform was removed in a vacuum chamber for 12 h. Lipids were diluted in PBS buffer to a concentration of 200 μg/ml before preparing small unilamellar liposomes by the sonication method. The lipid solution, kept on ice, was sonicated for 5 min with a VCX 500 model (Sonics and Materials, USA) equipped with a micro tip probe 421 (Misonix sonicator, USA). Power was adjusted to 200 W. After sonication, the solution was centrifuged at 10000 rpm for 5 min and the supernatant was transferred to a new tube. The average size of liposomes, 120 nm in diameter, was measured by dynamic light scattering (DLS) with a Zetasizer Nano ZS (Malvern Instruments Ltd, UK, He-Ne laser 633 nm). QSX303 silicon oxide sensors (Qsense, Sweden) were prepared according to the QSense procedure: extensive washing with a hellmanex 5% solution, rinsing with deionized water, drying under nitrogen flow. Sensors were finally activated with a plasma O_2 cleaner (Tespla, USA) for 5 min at 800 W. QCM-D chambers were first washed with PBS buffer at room temperature. The liposome solution was injected simultaneously in both chambers. A typical signal for SPB formation by liposome adsorption was obtained (see Fig. S2, Supplementary information). Following SPB formation on the sensor, QCM-D chambers were washed extensively with PBS buffer and temperature was brought to 30 °C.

2.5. QCM-D measurements

A Qsense E4 system and QSOFT software (Qsense, Sweden) were used for the QCM-D experiments. Two separate identical flow chambers (QFM 401) with POPC SPB were used for expression of eGFP and αHL-eGFP. The baseline of Δf and ΔD signals was reset to zero before injection of the cell-free reaction. The reactions were incubated 18 h. Δf and ΔD signals were recorded in real time with a data acquisition rate of 10 s^{-1}. After incubation, the QCM-D chambers were washed with PBS buffer. Best agreement between theory and experiments is obtained for resonance modes between 5th and 13th order. The 7th resonance frequency overtone was chosen for data analysis, since it is less sensitive to crystal mounting conditions according to the manufacturer. The 7th overtone corresponds to a frequency of 35 MHz (Qsense sensor has a resonance frequency of 4.95 MHz). A simplified version of the Sauerbrey equation [16] can be used with respect to the size (10 mm diameter) and type of crystal used in the study (QSX303). The additional mass per unit area $\Delta m = -(17.7/n) \times \Delta f$, where $n = 7$ (7th order), which gives a variation of 2.53 ng/cm^2 for a Δf of −1 Hz.

2.6. AFM images

An atomic force microscope Nanowizard 2 (JPK, Germany) mounted with OTR4 probes (Olympus, Japan) was used in contact

mode to image αHL-eGFP pores formed into POPC SPB. OTR4 probes were mounted on a JPK glass block system. After the cell-free reaction incubation, the sensor with the SPB was washed with PBS. Probes were immersed in the PBS above the sensor surface. The laser beam was manually aligned on the top of the AFM tip. The force applied on the sample, below 150 pN, was determined by the JPK routine procedure and adjusted while imaging. Images were recorded in different field of view, ranging from 5×5 μm to 512×512 nm with the same pixel resolution of 512×512. Frequency rate scanning was fixed to 4 Hz. Images were retreated using JPK imaging software. Vertical deflections data only are presented in this work.

3. Results and discussion

3.1. Cell-free expression of αHL-eGFP

In vitro transcription-translation was carried out in an *E. coli* cell-free extract using the endogenous RNA polymerase and sigma factor 70. A transcriptional activation cascade was used to express the αHL-eGFP fusion protein and eGFP. eGFP was used for control experiments. Genes encoding for both proteins (αHL-eGFP and eGFP) were cloned under a Ptar promoter [15] specific for the *E. coli* sigma factor 28 expressed in the first stage of the cascade (Fig. 1A). This activation mechanism introduces a delay of approximately 30 min before expression of the proteins. Synthesis of the fusion protein αHL-eGFP was confirmed by SDS PAGE (see Fig. S1, Supplementary information).

Activity of the pore-forming protein αHL-eGFP was verified by encapsulating the cell-free reaction inside large synthetic phospholipid vesicles using a procedure described elsewhere [2]. The large vesicles were formed into a feeding solution containing all of the necessary nutrients for transcription and translation. Expression of αHL-eGFP inside the vesicles was visualized by fluorescence microscopy (Fig. 1B). A net extension of expression inside vesicles was observed compared to test tube reactions (Fig. 1C). 8 μM of αHL-eGFP were produced in the vesicles after 40 h of incubation, ten times more than in a batch mode reaction. As described previously with another cell-free expression system [2], αHL-eGFP creates a selective permeability at the membrane that allows feeding the internal reaction with nutrients. In the test tube, the kinetics of expression was composed of the three phases commonly observed in cell-free reactions: a lag phase of 30 min due to the transcriptional activation cascade, the accumulation of the synthesized proteins in solution for a few hours and finally a plateau indicating the end of expression (Fig. 1C). Approximately 0.8 μM of αHL-eGFP were produced after 8 h of incubation, corresponding to 7.5 μg in a QCM-D chamber volume of 150 μl.

Pore formation was determined by comparing the protein production rate in batch mode and in large vesicles. In batch mode, the protein production rate is rapidly limited by the consumption of resources such as ATP. In large vesicles, the high protein production rate is maintained by feeding the reaction with nutrients. As expected, after 1 h of incubation the rate of protein production in large vesicles was greater than in cell-free reactions carried out in test tubes (inset Fig. 1C). Pore formation occurred no later than 1 h after the beginning of incubation at a maximum bulk concentration of 200 nM. α-hemolysin forms channels into phospholipid membranes within a few minutes at a monomer concentration as low as 2 nM [17]. For a 20 μm diameter vesicle, which is a non-limited diffusion scale, pore formation occurs at a maximum protein surface density of 400 μm^{-2} with a concentration in solution of

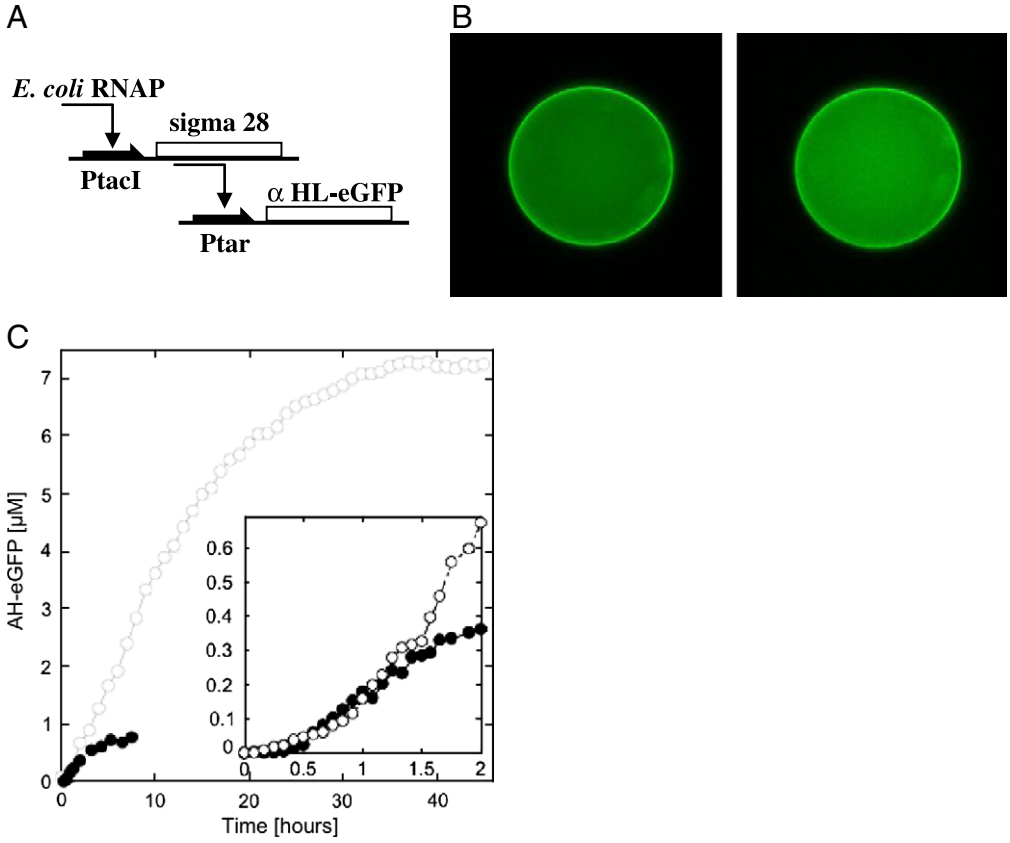

Fig. 1. Cell-free expression of αHL-eGFP. (A) Schematic of the transcriptional activation cascade. Sigma factor 28 was expressed from the sigma 70 promoter PtacI. The fusion protein αHL-eGFP was expressed from a Ptar promoter specific to sigma 28 (plasmid concentrations: 0.5 nM pBEST-sigma28, 5 nM pBEST-Ptar-UTR1-αHL-eGFP). (B) Cell-free expression of αHL-eGFP inside a large phospholipid vesicle. Fluorescence image after 3 h (left) and 6 h (right), scale bar: 10 μm. (C) Kinetics of αHL-eGFP expression in a large phospholipid vesicle measured by fluorescence (open circles) and in a test tube (filled circles). Inset: blow-up of the first 2 h of expression in vesicle (open circles) and in a test tube (filled circles).

200 nM. This estimation, which corresponds to a surface coverage of approximately 1%, is an upper limit considering that all the αHL-eGFP monomers produced in the vesicle are adsorbed on the membrane.

3.2. QCM-D measurements: Δf signals

Fluorescence microscopy, which measures the entire production of αHL-eGFP inside large vesicles, cannot be used to describe the interaction of the pore-forming protein with the membrane. The interaction of αHL-eGFP with the phospholipid bilayer was characterized with a QCM-D monitoring technique. A solution of small unilamellar POPC liposomes was injected into the QCM-D chambers to form the SPB. Stability of the Δ*f* signal was reached after 5 min, which is the typical time for SPB formation (see Fig. S2, Supplementary information). The Δ*f* signal measured, similar to the signals obtained in previous studies on SPB formation [18], indicates the sensor surface was fully covered by a homogenous POPC bilayer. After formation of the SPB, the QCM-D chambers were washed with PBS. Two cell-free reactions were injected in two separate chambers: one for the expression of eGFP and the other for the expression of αHL-eGFP. Cell-free reactions were prepared on ice and warmed to room temperature before adding the plasmids to express eGFP and αHL-eGFP. Expression of eGFP instead of αHL-eGFP was used to characterize the signal of a cell-free reaction on an SPB. After the addition of plasmids, 180 μl of reactions were injected in each of the QCM-D chambers. Changes in the 7th overtone resonant frequency of the sensor were recorded in real time over 18 h (Fig. 2).

A Δ*f* of −35 Hz to −45 Hz was observed in both chambers upon injection of the cell-free reactions (inset Fig. 2). After injection, the signals from each chamber displayed drastically different behaviors. The eGFP Δ*f* signal decreased to −60 Hz during the first 2 h, then increased for the next 5 h to a final Δ*f* of −40 Hz. Although no explanation could be provided, this non-specific adsorption-desorption on the SPB might be due to a pH change. It is known that the pH of batch mode cell-free reactions decreases by one unit over a few hours of expression [19], which can change the interactions of electrostatic nature between the proteins and the membrane. The Δ*f* signal returned to 0–5 Hz after the post-incubation washing step, indicating a negligible amount of material was still adsorbed on the SPB. The beginning of eGFP synthesis, which occurs after 30 min of incubation (Fig. 1C), was not marked by a change of the Δ*f* rate. As a comparison, a Δ*f* of a few Hz was measured for diluted protein solutions (50 μg/ml) on PC SPB, and a Δ*f* on the order of 10 Hz for fetal bovine serum solutions [12]. The cell-free expression reaction used in this study is a dense and viscous solution composed of 10 mg/ml of proteins as well as many of the components required for coupled transcription-translation such as tRNAs.

Signals obtained for eGFP, used as a background cell-free reaction, were subtracted from the signals obtained for αHL-eGFP. The Δ*f* for αHL-eGFP was characterized by two different regimes. After the 30 min lag phase due to the transcription cascade, the αHL-eGFP Δ*f* dropped abruptly to −150 Hz in the next 30 min (Fig. 2). After 1 h of incubation, the Δ*f* rate decreased by a factor of ten whereas the protein production in solution increased linearly (Fig. 1C). The Δ*f* dropped continuously during the entire incubation time. The Δ*f* signal reached −370 Hz after 18 h of incubation and the final washing step. This entire experiment (eGFP and αHL-eGFP) was repeated five times, including new SPB formation and new cell-free reaction preparation. The same signals were observed with a maximum of 15% variations in amplitudes across the experiments.

3.3. Mass added on the SPB

The mass of material adsorbed on the SPB can be estimated from Δ*f* with the Sauerbrey equation [16]. It is, however, difficult to determine the exact mass of αHL-eGFP adsorbed on the SPB. First, the mass measured by the QCM-D includes the water coupled to or trapped on the adlayer. Second, the Sauerbrey equation is valid below a Δ*D* of 1×10^{-6} per 10 Hz. For αHL-eGFP, the first regime is in this limit (Figs. 2 and 3). The second regime, after 1 h of incubation, is above this limit. Rather than determining the exact mass of αHL-eGFP adsorbed on the SPB, a lower limit and an upper limit of the mass is estimated based on the Sauerbrey equation and the following numbers: 61200 g/mol for the molar mass of the fusion protein, 10 mm for the sensor diameter, a pore diameter between 10 nm for α-hemolysin pores [20] and 16 nm for the αHL-eGFP heptamer (with an average size of 3 nm for eGFP). Arrangement of the circular heptamers in a close packed hexagonal lattice [21,22] covers 90% of the total surface area, 10% greater than a square lattice (80%). Taking into consideration the circular geometry of the pore, the maximum mass of αHL-eGFP pores that can be inserted into an SPB covering the entire sensor surface area is between 230 ng (square lattice, pore diameter 16 nm) and 660 ng (hexagonal lattice, pore diameter 10 nm). The remaining

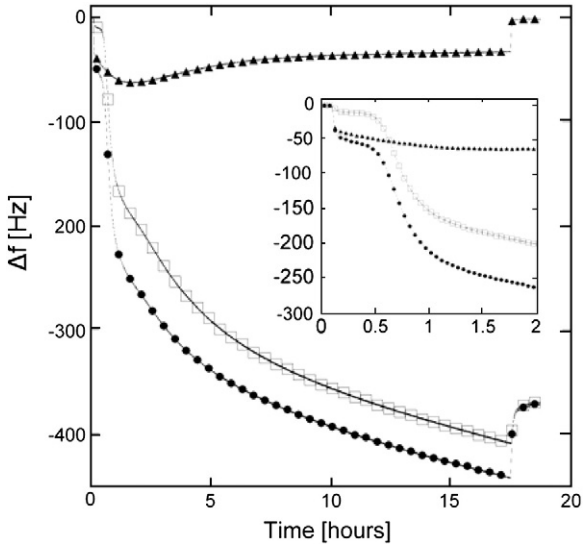

Fig. 2. Cell-free expression on an SPB in QCM-D chambers, Δ*f* signals. Cell-free expression of eGFP (filled triangles), αHL-eGFP (filled circles), subtraction of the eGFP signal from the αHL-eGFP signal (open squares). Inset: blow-up of the first 2 h.

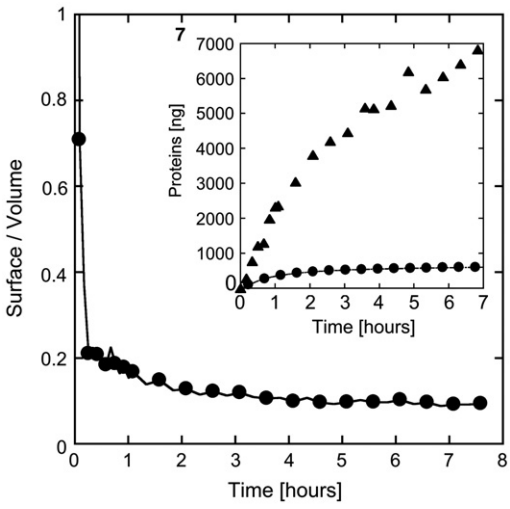

Fig. 3. Ratio of the mass of αHL-eGFP adsorbed on the SPB with the mass of αHL-eGFP synthesized in solution (QCM-D volume chamber 150 μl). The initial lag phase of 30 min was removed. Inset: mass of αHL-eGFP expressed in solution (filled triangles) and adsorbed on the SPB (filled circles).

free space, where αHL-eGFP monomers can adsorb without forming pores, is on the order of 10% of the total surface area for a hexagonal lattice and 20% for a square lattice. The maximum expected mass of αHL-eGFP adsorbed onto the SPB (pores and monomers) for the entire sensor surface area is between 250 ng (square lattice, pore diameter 16 nm, 80% of pores, 20% of monomers) and 730 ng (hexagonal lattice, pore diameter 10 nm, 90% pores, 10% monomers). It corresponds to a Δf between −125 Hz and −365 Hz based on the Sauerbey equation. In the case of proteins, an increase of mass by a factor of 1.5 to 3 is usually observed between dry and wet conditions due to the water coupled to the adlayer [23]. The total Δf was expected to fall between −190 Hz and −1100 Hz. In the case of αHL-eGFP, two frequency regimes were observed: a fast adsorption of mass, characterized by a frequency decrease of amplitude −150 Hz (from 0.5 h to 1 h of incubation, inset Fig. 2), followed by a slow adsorption of mass, characterized by a final Δf of −370 Hz after the final washing step. The experimental results, which fall into the lower part of the Sauerbrey estimation, indicate that a dense but not compact layer of large αHL-eGFP pores was formed in the SPB. This conclusion was confirmed later by AFM (Fig. 6).

The amount of αHL-eGFP expressed in solution, calculated from the fluorescence measurements for a chamber volume of 150 μl (Fig. 1C), was compared to the amount added to the bilayer (using the upper limit of 730 ng) after the lag phase of 30 min (Fig. 3). The rapid decrease of the Δf rate observed after 1 h of incubation ($\Delta f = -150$ Hz) occurred with a linear increase of protein concentration in solution and in large excess of the total protein amount.

3.4. QCM-D measurements: ΔD signals

In addition to Δf, the QCM-D technique provides a dissipation signal, which measures the attenuation of the mechanical oscillations. ΔD, the ratio between stored and dissipated energy, measures the change in the surface layer softness or stiffness [24–27]. In the case of eGFP, ΔD was proportional to Δf for the entire incubation period. ΔD reached a maximum of 35×10^{-6} after 2 h and stabilized at 22×10^{-6} after 7 h (Fig. 4A). ΔD returned to $2–3\times10^{-6}$ after the final washing step. Observations for eGFP are in good agreement with previous studies of protein adsorption on PC SPB [12]. When αHL-eGFP was expressed, for the first hour of incubation, ΔD was proportional to Δf. For the next 30 min of incubation, while Δf was increasing, no change in ΔD was observed (Fig. 4B). After 1.5 h of incubation, the dissipation resumed increasing proportional to Δf, but at a smaller rate. After the final rinsing step, ΔD returned to its value after 12 h of incubation. More material adsorbed on the SPB was removed during the rinsing step for αHL-eGFP than for eGFP.

The *D-f* curves (ΔD plotted against Δf) provide an alternative presentation of the QCM-D data. Low values of $\partial D/\partial f$, characteristic of a rigid layer, indicate an addition of mass without significant change in the dissipation. High values of the $\partial D/\partial f$, characteristic of a soft layer, correspond to a high dissipation per added mass. Variations of $\partial D/\partial f$ were observed for structural changes of proteins during adsorption, such as hemoglobin and BSA [25,26]. In the case of eGFP, a large $\partial D/\partial f$ was measured for both the adsorption and the desorption processes. Proteins from the extract adsorbed non-specifically on the membrane then partly desorbed after a few hours of incubation. No tight binding to the SPB was observed since the material adsorbed was almost entirely removed after the final rinsing step. In the case of αHL-eGFP, two distinct regimes were observed (Fig. 5A and B). In the first regime, from 0 to −190 Hz, a fast transition from a high dissipation per added mass to a low negative dissipation per added mass was measured. The fast adsorption of αHL-eGFP monomers on the SPB was followed by pore formation in the membrane, which was marked by a net change of the $\partial D/\partial f$. Both the change in $\partial D/\partial f$ and the change in the Δf rate after 1 h of incubation indicate that a dense layer of αHL-eGFP channels formed

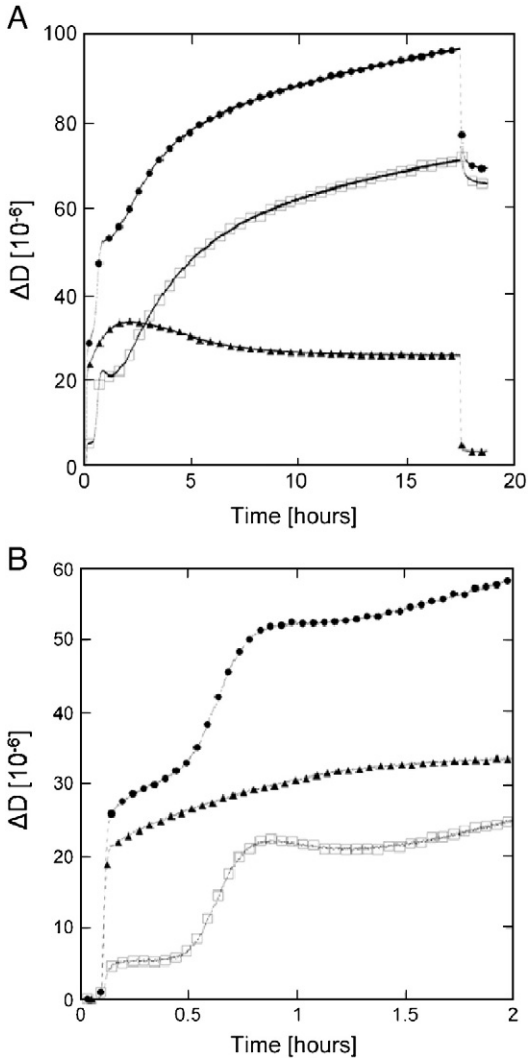

Fig. 4. Cell-free expression on an SPB into QCM-D chambers, ΔD signals. (A) Cell-free expression of eGFP (filled triangles), αHL-eGFP (filled circles), subtraction of the eGFP signal from the αHL-eGFP signal (open squares). (B) Blow-up of the first 2 h.

in the SPB between 0.5 and 1 h of incubation. Such dramatic changes in the viscoelastic properties of the membrane have been observed recently with smaller amplitude for the pure pore-forming peptide gramicidin D [13]. In the second regime, from −190 Hz to −370 Hz, ΔD increased almost linearly with the addition of mass. The fast formation of a dense layer of pores in the SPB was followed by the adsorption of a soft layer of material. This material, added in the second regime, was not entirely removed after the final washing step.

3.5. AFM observations

An AFM in liquid was used to image the SPB after cell-free expression of αHL-eGFP. An SPB was formed on a sensor outside the Qsense instrument. The cell-free reaction was incubated overnight on top of the pre-formed POPC bilayer. The sensor was rinsed with PBS before AFM imaging. All over the scanned surface donut-like structures of approximately 10–15 nm in diameter were imaged, consistent with the dimensions and geometry of α-hemolysin pores (Fig. 6). These structures could neither be observed in control experiment samples (expression of eGFP on POPC SPB) nor in POPC SPB only (data not shown). A high surface density of pores was observed in different locations on the SPB. Multiple OTR4 probes were used. None of our observations could be interpreted as possible imaging artifacts. Formation of two-dimensional hexagonal crystals of

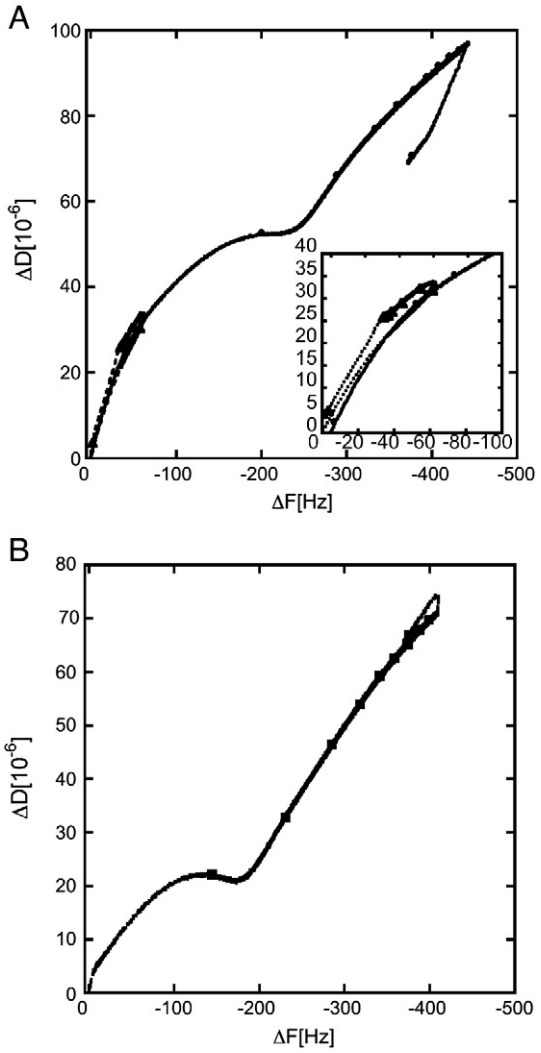

Fig. 5. Dissipation signal against the frequency signal (*D-f* plots). (A) Cell-free expression of eGFP (filled triangles) and αHL-eGFP (filled circles). Inset: blow-up from 0 to −100 Hz. (B) Corrected signal, eGFP signal subtracted from the αHL-eGFP signal (filled squares).

α-hemolysin channels have already been observed in SPB formed on mica surfaces [21,22]. Such structures could not be observed since silicon surfaces, which have a higher roughness (2–3 nm) than mica surfaces (100 pm), prevent formation of crystal structures and uniform imaging of the surface. In addition, the presence of eGFP in the C-terminal part of α-hemolysin may prevent crystal formation. Structures of a few tens of nanometers in size were also revealed randomly dispersed on the surface. These structures could explain the adsorption of soft material observed in the second regime after pore formation (Fig. 5B). Furthermore, the cell-free reaction was incubated above the sensor in an open environment, which may have favored accumulation and sedimentation of aggregates on the SPB. In the QCM-D instrument, the sensor is located on top of the chamber and solutions are passed below, reducing sedimentation.

3.6. QCM-D signals interpretation

Δ*f* signals observed for eGFP and αHL-eGFP can be divided into five parts (Fig. 7A and B). In the case of eGFP, the injection of the extract is characterized by a fast Δ*f* drop (part 1, Fig. 7A). An adsorption-desorption of cell-free material (essentially proteins) on the SPB is observed over a few hours (part 2 and 3). The signal is almost stable at −40 Hz for the last 10 h of incubation (part 4). In part 5, after the final rinsing step with PBS, the Δ*f* returns to 0–5 Hz, indicating a small amount of material remains adsorbed on the membrane. None of the components of the cell free reaction mixture seem to have a strong affinity with the POPC SPB.

In the case of αHL-eGFP, the injection of the extract results in the same fast Δ*f* drop as observed for eGFP (part 1, Fig. 7B). The lag phase (part 2) is followed by a massive formation of pores in the SPB (part 3), characterized by a fast and large Δ*f* and Δ*D*. Pore formation in the SPB is faster than in large vesicles since the surface to volume ratio is much larger in the QCM-D chamber. Whereas a frequency decrease of magnitude 150 Hz is observed in the first 30 min after the lag phase, a Δ*f* with same magnitude is observed over the last 17 h of incubation (part 4). The material added onto the SPB during this long incubation time is not entirely removed after the final rinsing step (part 5). The Δ*D* signal, proportional to the Δ*f* signal, and the *D-f* plots suggest material slowly adsorbs onto the SPB, which is almost fully covered by αHL-eGFP channels. This material adsorbs with no apparent structural change but with a relatively strong binding to the SPB. Although no clear explanation can be provided, interactions of αHL-eGFP monomers with channels could account for this addition of mass on the SPB.

3.7. Adsorption kinetics model

The QCM-D data suggest pore formation occurs during the first regime between 30 min and 60 min of incubation. After 1 h of incubation, the SPB is almost saturated with αHL-eGFP channels. In the second regime, the mass added onto the SPB does not seem to be directly related to the massive pore formation that occurs in 30 min. The simple model developed below focuses on pore formation in the SPB.

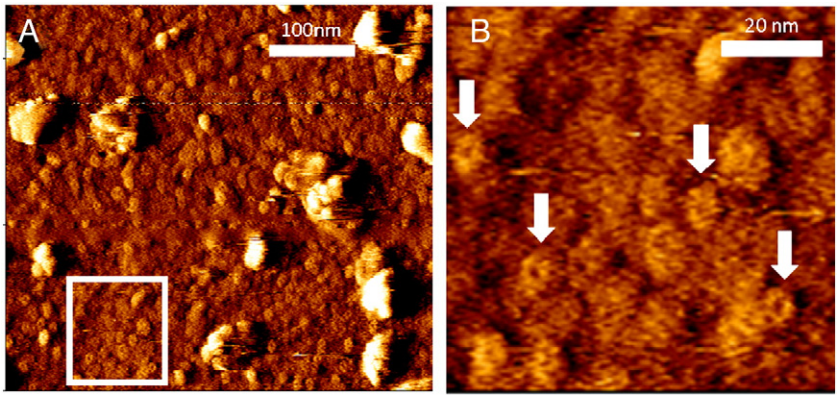

Fig. 6. AFM image in liquid medium of the SPB formed on the sensor surface after cell-free expression of αHL-eGFP and washing procedures. (A) 512×512 nm square image. (B) Blow-up of the white frame shown in A. Arrows point to αHL-eGFP pores.

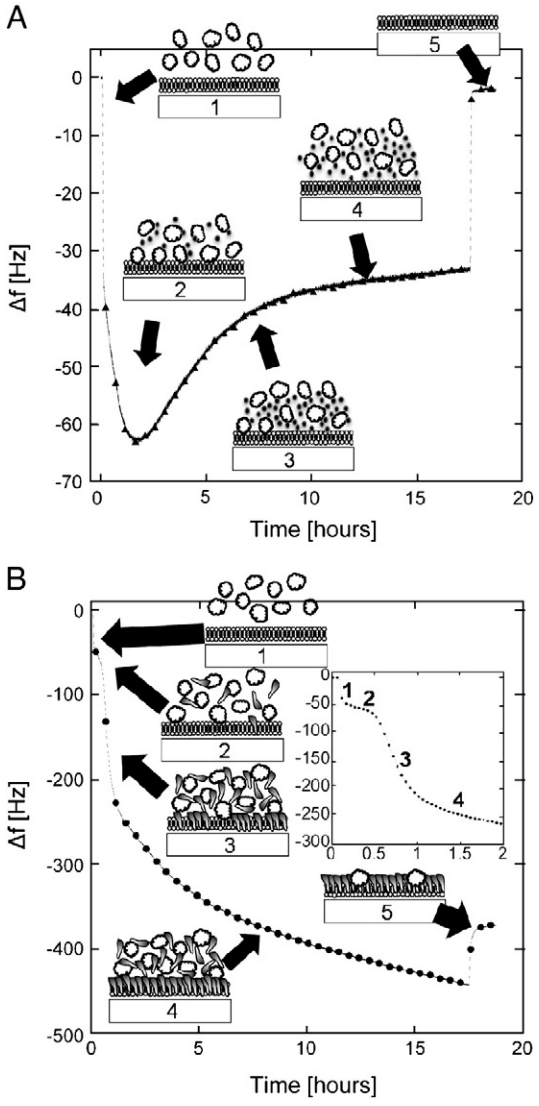

Fig. 7. Δf signals interpretation of cell-free expression on SPB. Cell-free extract components are shown as large particles, eGFP as small dots and αHL-eGFP as elongated shapes. (A) Cell-free expression of eGFP. (B) Cell-free expression of αHL-eGFP.

Many models have been proposed to describe the kinetics of protein adsorption on surfaces. The equations presented hereafter are based on the model developed by Corsel and coworkers for independent binding sites [28]. The surface coverage $\Gamma(t)$ is given by:

$$\frac{d\Gamma(t)}{dt} = k_{on}C(t)\left(1-\frac{\Gamma(t)}{\Gamma_{max}}\right)-k_{off}\Gamma(t) \quad (1)$$

where $\Gamma(t)$ is the mass adsorbed per unit surface at time t (ng/cm^2), k_{on} is the adsorption constant (cm/s), $C(t)$ the concentration of αHL-eGFP monomers close to the surface (ng/cm^3), k_{off} the desorption constant (s^{-1}) and Γ_{max} the maximum mass per unit surface. In the context of this study, the following hypotheses were made: the pore-forming protein binds irreversibly on the membrane, the surface area of a monomer is equal to the surface area of a monomer in the heptamer, the protein concentration at the surface is equal to the concentration in the bulk solution. The first hypothesis is supported by the strong and fast interaction of the pore-forming protein with the membrane. Furthermore, as estimated before, the critical surface density for pore formation is so low that the Δf measured corresponds rapidly to a mass of αHL-eGFP channels irreversibly anchored to the SPB. Although monomers change conformation upon channel formation, there is no significant change in the surface area occupied by one protein alone or in a heptamer. The second hypothesis is supported by the crystallographic structure of the channel [7]. In the last hypothesis, the concentration of monomers in solution close to the sensor surface is overestimated by equating it to the concentration in bulk far from the sensor surface. Concentration of monomers at the SPB surface depends on the mass transport. Due to the adsorption of αHL-eGFP monomers on the SPB, a diffusion gradient is formed from the surface to the bulk solution, which depends on time since the concentration of monomers in bulk is not constant. A lower limit on the value of k_{on} is found by taking the concentration of free monomers at the surface equal to the concentration in bulk. Eq. (1) can be re-written:

$$\frac{d\Gamma(t)}{dt} = k_{on}C(t)\left(1-\frac{\Gamma(t)}{\Gamma_{max}}\right) \quad (2)$$

The numerical solution of Eq. (2) is:

$$\Gamma(t) = \Gamma_{max}\left(1-e^{-\frac{k_{on}}{\Gamma_{max}}\int C(t)dt}\right) \quad (3)$$

Using the Sauerbey equation (Eq. (4)):

$$\Delta f(t) = -\left(\frac{n}{c}\right)\Delta m(t) = -\left(\frac{n}{c}\right)\Gamma(t) \quad (4)$$

Eq. (3) can be expressed in terms of the frequency change per centimeter squared:

$$\Delta f(t) = -f_{max}\left(1-e^{-\frac{k_{on}}{\Gamma_{max}}\int C(t)dt}\right) \quad (5)$$

with $f_{max} = (n/c)\ \Gamma_{max}$. To fit Eq. (5) to the frequency data, $C(t)$ was determined by a numerical fit of the fluorescence data (see Fig. S3, supplementary information), n = 7 (7th order of resonance), and the sensor sensibility c = 17.7 ng/(cm^2 Hz). The best fit was obtained for $f_{max} = -190$ Hz/cm^2 and an association constant $k_{on} = 43 \pm 1$ cm s^{-1}, or equivalently $k_{on} = 0.6 \times 10^7$ M^{-1} s^{-1} with a surface area per monomer of 25 nm^2 (Fig. 8). This value of k_{on} is a lower limit since $C(t)$ is overestimated. The same order of magnitude for k_{on} was obtained for the interaction of Prothrombin on phospholipid membranes [27],

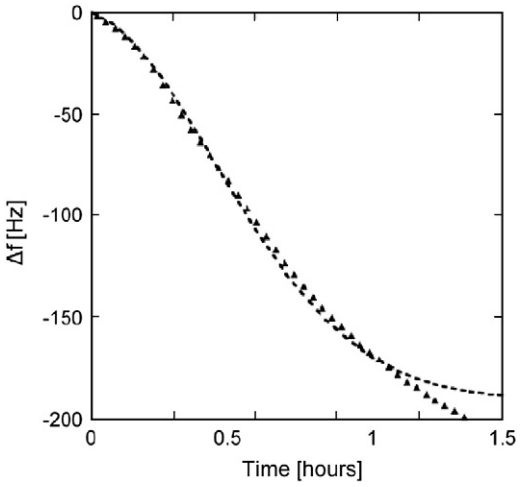

Fig. 8. Corrected Δf signal for αHL-eGFP (closed triangles, first 1.5 h) compared to the model (dashed line). The initial lag phase of 30 min was removed.

whereas k_{on} was ten to one hundred times smaller for the interaction of Annexin I with membranes [29].

4. Conclusions

New methodologies have to be developed to characterize membrane protein interactions and functions. Understanding membrane protein assembly is also important in order to make synthetic devices such as surface sensors composed of biological components. In this work, α-hemolysin, a model of pore-forming protein, was used to present a novel approach to study membrane interacting proteins. The concurrent cell-free expression and insertion of the protein into a phospholipid membrane was characterized by fluorescence microscopy and the QCM-D monitoring technique. Cell-free expression was used directly on an SPB to monitor real time pore formation with the QCM-D technique. Interaction of the cell-free synthesized protein with the membrane and changes in the viscoelastic properties of the lipidic bilayer were characterized by the Δf and the ΔD signals. Cell-free expression presents many advantages for membrane protein studies: it bypasses fastidious membrane protein preparation, it reproduces the native process of synthesis and insertion and it is an affordable technique.

In this work, we used phosphatidylcholine phospholipids because it is a major component of biological membrane and it is a typical lipid used in membrane studies. POPC SPB are easy to form [13] and they have been largely used in AFM studies. One of the interesting steps after this work would be to change the composition of the membrane to study the relationship between the phospholipid composition and the kinetics of pore formation. The approach presented in this work could be used to study the insertion of integral membrane proteins [6] or interactions between cytoplasmic and membrane proteins. Expression of multiple proteins at the same time has already been done [30]. Plasmid concentrations have to be adjusted to get the desired protein production. Elementary gene networks, such as transcriptional activation cascades, can be used to create time delays between the productions of different proteins. As for the interaction between a membrane protein and a cytoplasmic protein, inner membrane proteins would certainly adopt the correct orientation to study interaction with a cytoplasmic protein. A model system has yet to be defined.

Acknowledgments

QCM-D experiments and AFM Imaging were performed at the Institut des Technologies Avancées en Sciences du Vivant (Toulouse, France). This work was supported by the grant ANR-09-PNANO-P150-36 and the NSF grant PHY-0750133. Jerome Chalmeau is supported by the DGA (Direction Generale de l'Armement) Abroad Post doctoral program PDE 09C0023. Vincent Noireaux thanks Catherine Raach for reading and correcting the manuscript.

Appendix A. Supplementary data

Supplementary data to this article can be found online at doi:10.1016/j.bbamem.2010.07.027.

References

[1] M. He, Cell-free protein synthesis: applications in proteomics and biotechnology, N. Biotechnol. 25 (2008) 126–132.
[2] V. Noireaux, A. Libchaber, A vesicle bioreactor as a step toward an artificial cell assembly, Proc. Natl Acad. Sci. USA 101 (2004) 17669–17674.
[3] H. Bayley, B. Cronin, A. Heron, M.A. Holden, W.L. Hwang, R. Syeda, J. Thompson, M. Wallace, Droplet interface bilayers, Mol. Biosyst. 4 (2008) 1191–1208.
[4] R. Robelek, E.S. Lemker, B. Wiltschi, V. Kirste, R. Naumann, D. Oesterhelt, E.K. Sinner, Incorporation of in vitro synthesized GPCR into a tethered artificial lipid membrane system, Angew. Chem. Int. Ed Engl. 46 (2007) 605–608.
[5] N.T. Hovijitra, J.J. Wuu, B. Peaker, J.R. Swartz, Cell-free synthesis of functional aquaporin Z in synthetic liposomes, Biotechnol. Bioeng. 104 (2009) 40–49.
[6] F. Katzen, T.C. Peterson, W. Kudlicki, Membrane protein expression: no cells required, Trends Biotechnol. 27 (2009) 455–460.
[7] L. Song, M.R. Hobaugh, C. Shustak, S. Cheley, H. Bayley, J.E. Gouaux, Structure of staphylococcal alpha-hemolysin, a heptameric transmembrane pore, Science 274 (1996) 1859–1866.
[8] R. Richter, A. Mukhopadhyay, A. Brisson, Pathways of lipid vesicle deposition on solid surfaces: a combined QCM-D and AFM study, Biophys. J. 85 (2003) 3035–3047.
[9] F.F. Rossetti, I. Reviakine, G. Csucs, F. Assi, J. Voros, M. Textor, Interaction of poly(L-lysine)-g-poly(ethylene glycol) with supported phospholipid bilayers, Biophys. J. 87 (2004) 1711–1721.
[10] S. Tombelli, M. Minunni, E. Luzi, M. Mascini, Aptamer-based biosensors for the detection of HIV-1 Tat protein, Bioelectrochemistry 67 (2005) 135–141.
[11] K. Otto, T.J. Silhavy, Surface sensing and adhesion of *Escherichia coli* controlled by the Cpx-signaling pathway, Proc. Natl Acad. Sci. USA 99 (2002) 2287–2292.
[12] K. Glasmastar, C. Larsson, F. Hook, B. Kasemo, Protein adsorption on supported phospholipid bilayers, J. Colloid Interface Sci. 246 (2002) 40–47.
[13] E. Briand, M. Zach, S. Svedhem, B. Kasemo, S. Petronis, Combined QCM-D and EIS study of supported lipid bilayer formation and interaction with pore-forming peptides, Analyst 135 (2010) 343–350.
[14] J. Shin, V. Noireaux, Efficient cell-free expression with the endogenous *E. coli* RNA polymerase and sigma factor 70, J. Biol. Eng. 4 (2010) 8.
[15] D.N. Arnosti, M.J. Chamberlin, Secondary sigma factor controls transcription of flagellar and chemotaxis genes in *Escherichia coli*, Proc. Natl Acad. Sci. USA 86 (1989) 830–834.
[16] G. Sauerbrey, Verwendung von Schwingquarzen zur Wägung dünner Schichten und zur Mikrowägung, Z. Angew. Phys. 155 (1959) 206–222.
[17] A. Hildebrand, M. Pohl, S. Bhakdi, *Staphylococcus aureus* alpha-toxin–dual mechanism of binding to target-cells, J. Biol. Chem. 266 (1991) 17195–17200.
[18] C.A. Keller, B. Kasemo, Surface specific kinetics of lipid vesicle adsorption measured with a quartz crystal microbalance, Biophys. J. 75 (1998) 1397–1402.
[19] K.A. Calhoun, J.R. Swartz, Energizing cell-free protein synthesis with glucose metabolism, Biotechnol. Bioeng. 90 (2005) 606–613.
[20] L. Song, M.R. Hobaugh, C. Shustak, S. Cheley, H. Bayley, J.E. Gouaux, Structure of staphylococcal alpha-hemolysin, a heptameric transmembrane pore, Science 274 (1996) 1859–1866.
[21] Y. Fang, S. Cheley, H. Bayley, J. Yang, The heptameric prepore of a staphylococcal alpha-hemolysin mutant in lipid bilayers imaged by atomic force microscopy, Biochemistry 36 (1997) 9518–9522.
[22] D.M. Czajkowsky, S. Sheng, Z. Shao, Staphylococcal alpha-hemolysin can form hexamers in phospholipid bilayers, J. Mol. Biol. 276 (1998) 325–330.
[23] E. Reimhult, C. Larsson, B. Kasemo, F. Hook, Simultaneous surface plasmon resonance and quartz crystal microbalance with dissipation monitoring measurements of biomolecular adsorption events involving structural transformations and variations in coupled water, Anal. Chem. 76 (2004) 7211–7220.
[24] F. Hook, M. Rodahl, P. Brzezinski, B. Kasemo, Energy dissipation kinetics for protein and antibody–antigen adsorption under shear oscillation on a quartz crystal microbalance, Langmuir 14 (1998) 729–734.
[25] F. Hook, M. Rodahl, B. Kasemo, P. Brzezinski, Structural changes in hemoglobin during adsorption to solid surfaces: effects of pH, ionic strength, and ligand binding, Proc. Natl Acad. Sci. USA 95 (1998) 12271–12276.
[26] A.A. Feiler, A. Sahlholm, T. Sandberg, K.D. Caldwell, Adsorption and viscoelastic properties of fractionated mucin (BSM) and bovine serum albumin (BSA) studied with quartz crystal microbalance (QCM-D), J. Colloid Interface Sci. 315 (2007) 475–481.
[27] J.L. Jordan, E.J. Fernandez, QCM-D sensitivity to protein adsorption reversibility, Biotechnol. Bioeng. 101 (2008) 837–842.
[28] J.W. Corsel, G.M. Willems, J.M.M. Kop, P.A. Cuypers, W.T. Hermens, The role of intrinsic binding rate and transport rate in the adsorption of prothrombin, albumin, and fibrinogen to phospholipid-bilayers, J. Colloid Interface Sci. 111 (1986) 544–554.
[29] K. Kastl, M. Ross, V. Gerke, C. Steinem, Kinetics and thermodynamics of annexin A1 binding to solid-supported membranes: a QCM study, Biochemistry 41 (2002) 10087–10094.
[30] V. Noireaux, R. Bar-Ziv, A. Libchaber, Principles of cell-free genetic circuit assembly, Proc. Natl Acad. Sci. USA 100 (2003) 12672–12677.